

Reducing anomalous reflection from complex absorbing potentials: A semiclassical approachMicheline B. Soley ^{1,2,3} Kobra N. Avanaki ⁴ and Eric J. Heller⁴¹*Department of Chemistry and Chemical Biology, Harvard University, 12 Oxford Street, Cambridge, Massachusetts 02138, USA*²*Yale Quantum Institute, Yale University, P.O. Box 208334, New Haven, Connecticut 06520, USA*³*Department of Chemistry, Yale University, 225 Prospect Street, New Haven, Connecticut 06520, USA*⁴*Department of Physics and Department of Chemistry and Chemical Biology, Harvard University, Cambridge, Massachusetts 02138, USA*

(Received 22 August 2020; accepted 10 March 2021; published 6 April 2021; corrected 21 April 2021)

Numerical simulations are frequently required for quantum scattering problems and often face difficulties with finite grids and unwanted, unphysical reflections. For decades, improved complex absorbing potentials (CAPs) have been sought. Today, the rise of ultracold physics makes a solution essential as CAP errors increase at lower energies. We present a method that provides a physical, semiclassical picture of how to improve CAPs based on the behavior of classical trajectories. The method does not rely on the mathematical formalism often required by existing methods and reduces the error associated with CAP-based calculation of the low-energy scattering wavefunctions by up to several orders of magnitude relative to the standard Woods-Saxon approach, as demonstrated via the distorted-wave Born approximation. This indicates the method may be applied to the numerical simulation of collisions in the ultracold regime.

DOI: [10.1103/PhysRevA.103.L041301](https://doi.org/10.1103/PhysRevA.103.L041301)

Simulations of a wide variety of open systems [1] from chemical reactions [2] to cold and ultracold collisions [3–5] rely on complex absorbing potentials (CAPs or optical potentials). Although CAPs are designed to absorb the wavefunction in a region of position space, they are known to cause unphysical reflection effects in which low-energy components of the wave packet move counter to the expected direction and are not fully absorbed. This reflection problem has plagued quantum scattering and wave-packet propagation simulations for the past 30 years [6–9] and is especially troublesome today in cold and ultracold systems given the proportion of low-energy components of wave packets [3]. A solution to this problem would enable the study of ultracold collisions currently beyond reach due to the errors and computational intensity associated with existing CAPs.

A multitude of CAPs have been developed, including Woods-Saxon [10–12], linear negative imaginary [9,13], negative complex [7,14,15], energy dependent [16–19], channel dependent [20], parametrized and optimized [18,20–24], multihump imaginary [25], and wavefunction-ansatz based [26–28]. These methods are beneficial to specific systems, but face difficulties in the simulation of highly multidimensional low-energy systems. Absorption of the long-wavelength wavefunctions associated with low-energy systems often entails simulation of a broad range of position space via a large basis state or many grid points. Yet, the range of position space that can be simulated is limited due to the “curse of dimensionality” in which the size of the Hilbert space grows exponentially with the number of degrees of freedom.

Our approach takes these concerns into account. The method does not rely on mathematical formalism. Instead, it provides a physical understanding of how to improve CAPs based on classical trajectories and is straightforward to implement.

Since reflection is greater at lower energies, we carefully accelerate the particles with a negative real potential with corrections before they reach the imaginary potential. This reduces reflection while avoiding the need for added grid points. To prevent reflection from the hybrid potential, we add a term that ensures full absorption of particles with the lowest energy under study. Therefore, the method “reels in” and traps particles in the complex absorbing potential.

Our method relies on the disparate behavior of quantum and classical particles in a CAP. Quantum particles artificially reflect due to impedance mismatch if either the real or the imaginary part of the CAP changes too quickly relative to the particle’s wavelength (i.e., “quantum reflection” occurs when the Wentzel-Kramers-Brillouin (WKB) approximation fails even if the energy is above any potential barriers [29–31]). In the same potential, classical particles do not reflect. This suggests unphysical reflection from CAPs is reduced if quantum trajectories are made to behave more classically. We use this insight to reduce error in CAP simulations with semiclassical mechanics, which represent wavefunctions in terms of a sum over classical trajectories, as follows.

Semiclassically corrected complex absorbing potential. We first reduce reflection from the imaginary, absorbing part of the CAP. Since reflection from this part of the CAP occurs due to impedance mismatch between the CAP and the particle, reflection is expected to be greatest when the CAP is sharp relative to the particle, i.e., when the particle has low momentum. Error is reduced by speeding up the low-momentum components of the wave packet by slowly turning on a negative, real, smooth potential to the CAP [7,14]. The ideal real potential does not itself cause any reflection, such that quantum and classical trajectories behave equivalently. We find an attractive Coulomb potential correction fits the bill, as shown

below:

$$\begin{aligned} V_{\text{Coul corr}}(x) &= V_{\text{exp}}(x)V_{\text{Coul}}(x), \\ V_{\text{exp}}(x) &= \frac{V_0}{1 + e^{-\alpha(x-x_0)}}, \\ V_{\text{Coul}}(x) &= \frac{1}{(x-x_C)}, \end{aligned} \quad (1)$$

where V_{exp} is an exponential switching function of depth V_0 , width α , and position x_0 , and V_{Coul} is a Coulomb potential of position x_C . To avoid introduction of a singularity, the Coulomb potential V_{Coul} is situated beyond the upper limit of the position space domain at $x_C \geq x_{\text{max}}$.

The positions x_C and x_0 are chosen to lie just beyond and just before the imaginary potential to define a narrow speedup area near the absorbing region. An intermediate value is used for the width parameter α so that the Coulomb potential switches on slowly while the overall correction remains negligible in the interaction region. One way to select the depth V_0 is to determine the badlands condition [29,30,32–34], which ensures the accuracy of the semiclassical approximation, in the absorbing region. This provides a way to verify that the Coulomb potential yields the required acceleration while reducing the need for convergence calculations.

The three-dimensional Coulomb potential is shown to yield the same behavior classically and quantum mechanically through consideration of its Hamiltonian [35]

$$H = \frac{\mathbf{p}^2}{2m} + \frac{Ze^2}{r}, \quad (2)$$

where \mathbf{p} is the momentum, Z is the atomic charge, e is the electron charge, and r is the distance between the colliding particles. This Hamiltonian can be mapped to the Hamiltonian of a system of harmonic oscillators,

$$H = \sum_{i=1}^4 \left(\frac{P_i^2}{8m} - EX_i^2 \right) + Ze^2, \quad (3)$$

via extension of Cartesian space (\mathbf{x}, \mathbf{p}) to four dimensions and regularization with the Kustaanheimo-Stiefel transformation [36]

$$r = \sqrt{\sum_{i=1}^4 x_i^2} = \sum_{i=1}^4 X_i^2, \quad P_i = \sum_{j=1,4} p_j \frac{\partial x_j}{\partial X_i}, \quad d\tau = \frac{dt}{r} \quad (4)$$

$$x_1 = X_1^2 - X_2^2, \quad x_2 = 2X_1X_2, \quad (5)$$

$$x_3 = X_3^2 - X_4^2, \quad x_4 = 2X_3X_4, \quad (6)$$

where t and τ are the time and pseudotime, respectively [35]. Since the quantum pseudotime propagator is semiclassically exact for harmonic oscillators, and the Coulomb potential and the system of harmonic oscillators are equivalent, the Coulomb potential is accurately treated with the semiclassical pseudotime propagator as well. This propagator depends only on quantities derived from classical trajectories such that the quantum and classical results are equivalent, and therefore reflection free, at all energies [35,37,38].

We then address reflection from the switching potential $V_{\text{exp}}(x)$ that, unlike the Coulomb potential, is not guaranteed

to be reflection free. If the gradient of the switching function with respect to the position is too great relative to the particle wavelength, impedance mismatch arises from the real part of the potential that corresponds to the switching function, which leads to reflection from the real part of the potential. A traditional way to get rid of this error would be to broaden the switching function, but this would increase the amount of position space needed to simulate the CAP, which would in turn increase the cost of the simulation. Instead, we correct the CAP locally by adding a term that ensures that semiclassical and quantum amplitudes are equal at a given energy of interest, E .

Specifically, an adaptation of the strategy used by Maitra and Heller [39] is used to make the WKB wavefunction an exact solution of the Schrödinger equation:

$$\begin{aligned} 0 &= \left(-\frac{\hbar^2}{2m} \frac{d^2}{dx^2} + V_{\text{corr CAP}}(x, E) \right. \\ &\quad \left. + V_{\text{WKB corr}}(x, E) - E \right) \psi_{\text{WKB}}^{\pm}(x). \end{aligned} \quad (7)$$

Here $V_{\text{corr CAP}}$ is the Coulomb-corrected CAP of the form

$$V_{\text{corr CAP}}(x) = V_{\text{uncorr CAP}}(x) + V_{\text{Coul corr}}(x), \quad (8)$$

where $V_{\text{uncorr CAP}}$ is the uncorrected CAP, $V_{\text{Coul corr}}$ is the Coulomb correction [Eq. (1)], and $V_{\text{WKB corr}}$ is the ‘‘WKB correction’’ determined as follows:

$$\begin{aligned} V_{\text{WKB corr}}(x, E) &= -\hbar^2 \left[\frac{5}{32m} \left(\frac{V'_{\text{corr CAP}}(x)}{E - V_{\text{corr CAP}}(x)} \right)^2 \right. \\ &\quad \left. + \frac{V''_{\text{corr CAP}}(x)}{8m(E - V_{\text{corr CAP}}(x))} \right]. \end{aligned} \quad (9)$$

Note the scattering potential V_{PES} is not included in the WKB corrections, as reflection from this potential is physical and only artificial reflection from the CAP should be eliminated.

Although these perturbations can cause small reflections at energies other than E , they ensure the solution faces no impedance mismatch from either the real or imaginary potential at the specific energy of concern given the reflection-free nature of the semiclassical WKB solution, as discussed below.

We consider the WKB solution for a general potential energy surface V [40–43] as

$$\psi_{\text{WKB}}^{\pm}(x) = \frac{1}{\sqrt{|p(x, E)|}} \exp\left(\pm \frac{i}{\hbar} \int^x dx' p(x', E)\right), \quad (10)$$

where $p(x, E) = \sqrt{2m(E - V(x))}$, x , m , and E are the momentum, position, reduced mass, and energy, respectively. The WKB solution is given by two classical quantities: the square root of the classical probability density provides the prefactor and the classical action provides the argument of the exponent. As in the Coulomb case, since the WKB solution depends only on the classical trajectories that do not reflect, it cannot reflect in the absence of a barrier.

This approach offers a way to interpret CAP methods physically. In one dimension, where the Coulomb potential is not reflection free, wavefunctions are nonetheless accurately modeled with semiclassical WKB wavefunctions at long range; the WKB assumptions only fail within a finite

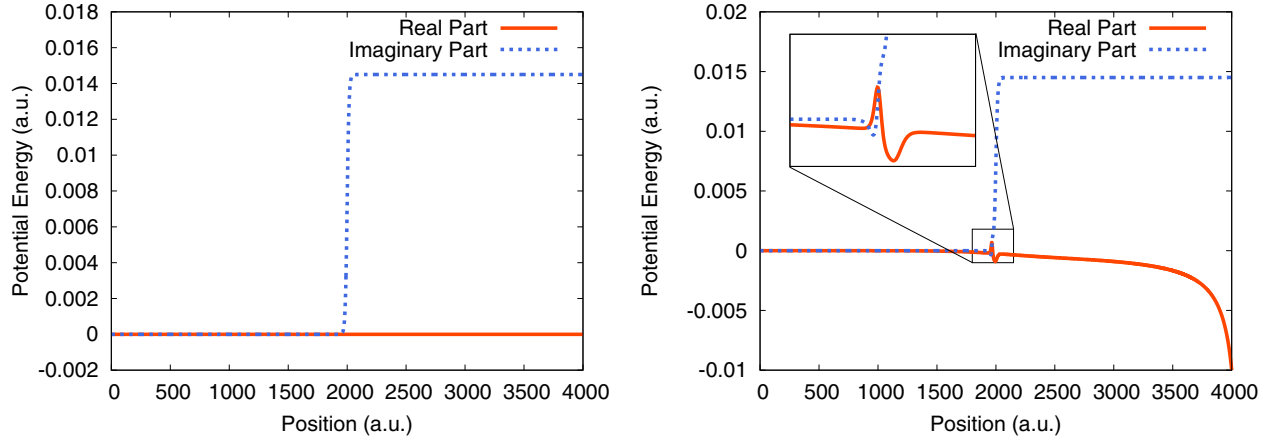


FIG. 1. Left: Real (orange solid line) and imaginary (blue dashed line) parts of the uncorrected Woods-Saxon complex absorbing potential $V_{\text{uncorr CAP}}$ [Eq. (11)] for parameters $V_d = 0.0145$ a.u., $x_m = 2000$ a.u., and $x_w = 8.0$ a.u. Right: Real (orange solid line) and imaginary (blue dashed line) parts of the corrected complex absorbing potential $V_{\text{corr CAP}}$ [Eq. (8)] with WKB corrections $V_{\text{WKB corr}}$ [Eq. (9)] (magnified in inset) defined at energy $E = 10^{-6}$ a.u. ($\equiv 316$ mK). Here we used $V_0 = 1.0$ a.u., $\alpha = 0.005$ a.u., $x_0 = 2000$ a.u., and $x_C = 4100$ a.u.

distance from the center of the Coulomb potential [30,44]. On the surface, the WKB corrections have similar form to those based on complex smooth exterior scaling [16,17,19] and Jost functions [45–47]. Yet, they differ significantly in that here corrections rely on classical trajectories. Physically, the corrections ensure wavefunctions behave classically (and therefore do not reflect) in the absorbing region of the potential, which promotes unit transmission through the CAP at that energy.

Distorted-wave Born approximation. Now we consider the addition of the semiclassical corrections to a common form of complex absorbing potential, the Woods-Saxon potential [12], which is defined as follows:

$$V_{\text{uncorr CAP}}(x) = i \left(V_d - \frac{V_d}{1 + e^{\frac{(x-x_m)}{x_w}}} \right). \quad (11)$$

In order to demonstrate how well the corrections reduce reflection, we employ potential parameters V_d , x_m , and x_w , which control the depth, position, and width, respectively. We choose parameters that artificially yield a CAP with a sharp onset and a small absorbing region to encourage much reflection at low energy as a benchmark. The parameters of the Coulomb correction are chosen so that the particles speed up before they reach the imaginary potential, thus reflecting negligibly. Here a broad Coulomb potential correction is employed; however, the length of the CAP region could be further reduced provided it sufficiently accelerates the particle away from the WKB correction region. The aforementioned badlands condition [29,30,32–34] may provide a way to quantify how much the Coulomb correction can reduce the required length of the simulated grid in CAP-based calculations. The WKB correction parameters are set at the lowest required energy, where the most reflection is expected. The resulting uncorrected and corrected CAPs are shown in Fig. 1.

We first investigate the reflection from the corrected CAP in a free particle collision of reduced mass $m = 1$ a.u., since

in that system the only reflection is artificial as there is no physical reflection from the system potential energy surface $V_{\text{PES}} = 0$. The method is then applied to a realistic system to demonstrate the method’s applicability to ultracold collisions. We determine the degree of transmission in a neutral potassium-potassium collision, modeled by the Morse potential:

$$V_{\text{PES}}(x) = D_e(1 - e^{-a(x-x_e)})^2 - D_e, \quad (12)$$

where $D_e = 0.0200725$ a.u. is the dissociation energy [48,49], $x_e = 7.47576$ a.u. is the equilibrium interatomic distance [50], $a = \sqrt{4mE_{\text{ZPE}}^2/(2D_e)}$ is the Morse potential parameter, $E_{\text{ZPE}} = 0.000209592$ a.u. is the zero-point energy [50], and $m = 35635.9$ a.u. is the reduced mass.

To evaluate the degree of reflection from the CAP at each energy, the proportion of the scattered wavefunction [the reflection coefficient $\mathcal{R}(E')$] is calculated according to the expression

$$\mathcal{R}(E') = \frac{\sigma_{\text{refl}}(E')}{\sigma_{\text{trans}}(E') + \sigma_{\text{refl}}(E')}, \quad (13)$$

where $\sigma_{\text{refl}}(E')$ is the reflection probability and $\sigma_{\text{trans}}(E') = 1$ is the transmission probability. Since the WKB solution exactly solves the Schrödinger equation when WKB corrections are used and by assumption the difference between the WKB-corrected potential and the original potential is small, the distorted-wave Born approximation is used to evaluate the scattering cross section perturbatively as follows [39,51–53]:

$$\sigma_{\text{refl}}(E') = \frac{m^2}{\hbar^2} \left| \int_{-\infty}^{\infty} dx U(x, E, E') \frac{e^{(2i/\hbar) \int^x dx' p(x')}}{p(x)} \right|^2, \quad (14)$$

where here the momentum p is approximated as $\sqrt{2mE}$ for energies $|E - V(x)| < 10^{-9}$ a.u. to avoid numerical instability. Here the perturbation $U(x, E, E')$ transforms the Hamiltonian exactly solved by the WKB wavefunction at energy E into the Hamiltonian of the potential under

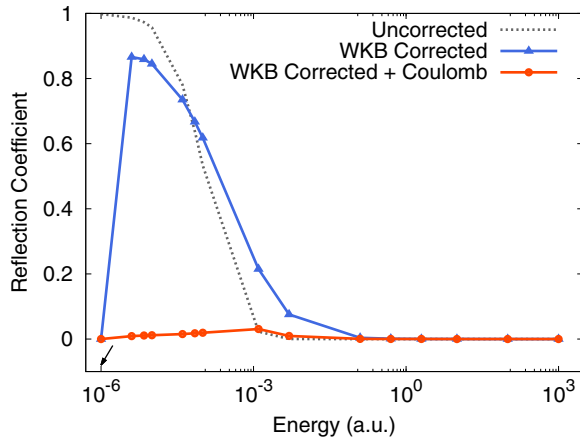


FIG. 2. The corrected CAP [Eq. (8)] (orange solid line with circles) significantly reduced reflection for the free-particle collision as compared to the uncorrected CAP [Eq. (11)] (gray dashed line) and the WKB corrected CAP [Eq. (9)] (blue solid line with triangles) defined at energy $E = 10^{-6}$ a.u. (equivalent to 316 mK, marked with arrow). Quadrature was performed in the position space region $x \in [0, 4000]$ a.u. with 2^{16} equal grid points.

study at energy E' . We calculate the reflection coefficient for three different CAPs: the uncorrected CAP $V_{\text{uncorr CAP}}$, the WKB corrected CAP $V_{\text{uncorr CAP}} + V_{\text{WKB corr}}$ (similar to Refs. [16,46]), and the fully corrected CAP $V_{\text{corr CAP}}$. For realistic scattering systems, we determine the degree of artificial reflections from the CAPs via calculation of the error in the transmission coefficient $1 - \mathcal{R}(E')$ relative to that of the physical scattering potential V_{PES} . We evaluate the reflection coefficient at low energy, where reflection is expected to be highest, and over several magnitudes of energy, given the energy uncertainty inherent in wave-packet dynamics.

As expected, the corrected CAP successfully reduced reflection by several orders of magnitude at low energies relative to the uncorrected CAP in the absence of real, physical reflection, as illustrated in Fig. 2. At the lowest energy considered, $E' = E$, the uncorrected CAP reflected nearly all the wavefunction and the WKB corrections completely eliminated reflection. The addition of Coulomb potential corrections reduced reflection by an order of magnitude relative to WKB corrections alone at all energies tested.

The form of the reflection coefficient of the WKB corrected CAPs (blue solid line with triangles and orange solid line with circles) can be understood with a physical picture that relates classical and quantum behaviors. At the energy of the WKB corrections, the particle behaves classically, and there is no reflection. As the energy increases, the corrections are no longer exact and quantum reflection reemerges until reflection reaches a maximum. Finally, reflection decreases again as the system approaches the classical limit.

The corrections also significantly improved the accuracy of the calculated transmission coefficient for the realistic model of a low-energy collision shown in Fig. 3. The WKB corrections eliminated error at the lowest energy under consideration (10^{-11} a.u. $\approx 3.16 \mu\text{K}$), and the addition of the Coulomb correction further reduced error to near zero at all energies under study.

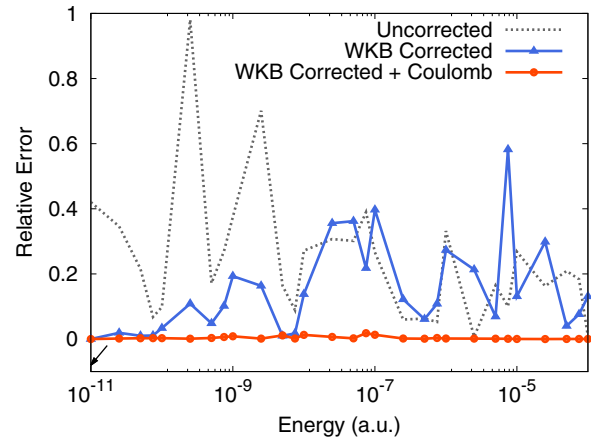


FIG. 3. For the benchmark ultracold collision calculation [Eq. (12)], the corrected CAP [Eq. (8)] (orange solid line with circles, $V_0 = 1$ a.u., $\alpha = 0.5$ a.u., $x_0 = 200$ a.u., $x_C = 410$ a.u.) determined the transmission coefficient with higher accuracy than the uncorrected CAP [Eq. (11)] (gray dashed line, $V_d = 0.0145$ a.u., $x_m = 375$ a.u., and $x_w = 0.1$ a.u.) and the WKB-corrected CAP [Eq. (9)] (blue solid line with triangles, fixed at energy $E = 10^{-11}$ a.u. $\approx 3.16 \mu\text{K}$ as indicated by an arrow). Quadrature was performed for 2^{12} equally spaced grid points in the position space region $x \in [0, 400]$ a.u.

This semiclassical method reduces the error associated with artificial reflections in CAPs by orders of magnitude at low energy. Using a physical picture of reeling in low-momentum particles and eliminating reflection at the lowest energy of interest was found to be more accurate than the WKB approach alone. This result indicates the method may be used to simulate real systems such as ultracold collisions, where existing solutions are inaccurate and/or expensive. Since this CAP absorbs the wavefunction over a broad range of energy, it may prove to be useful for absorbing multidimensional wave packets, which reach the CAP wall with widely different proportions of the total energy. The method also decreases the amount of position space that must be simulated with the use of local corrections, which would be especially beneficial in highly multidimensional systems that face the curse of dimensionality. This indicates the method shows promise for simulation of systems previously beyond reach.

Financial support was provided by the National Science Foundation Grant No. DGE-1144152, the Harvard Graduate School of Arts and Sciences Merit/Graduate Society, the Blue Waters Graduate Research Fellowship, and the Yale Quantum Institute Postdoctoral Fellowship. This research is part of the Blue Waters sustained-petascale computing project, which is supported by the National Science Foundation (Awards No. OCI-0725070 and No. ACI-1238993), the state of Illinois, and as of December 2019, the National Geospatial-Intelligence Agency. Blue Waters is a joint effort of the University of Illinois at Urbana-Champaign and its National Center for Supercomputing Applications. We thank Prof. V. S. Batista for helpful discussions.

- [1] J. G. Muga, J. P. Palao, B. Navarro, and I. L. Egusquiza, Complex absorbing potentials, *Phys. Rep.* **395**, 357 (2004).
- [2] A. Ben-Asher and N. Moiseyev, Complex absorbing potentials for stark resonances, *Int. J. Quantum Chem.* **120**, e26067 (2020).
- [3] J. Huang, S. Liu, D. H. Zhang, and R. V. Krems, Time-Dependent Wave Packet Dynamics Calculations of Cross Sections for Ultracold Scattering of Molecules, *Phys. Rev. Lett.* **120**, 143401 (2018).
- [4] V. Kokoouline, O. Dulieu, R. Kosloff, and F. Masnou-Seeuws, Theoretical treatment of channel mixing in excited Rb₂ and Cs₂ ultracold molecules: Determination of predissociation lifetimes with coordinate mapping, *Phys. Rev. A* **62**, 032716 (2000).
- [5] T. Laue, P. Pellegrini, O. Dulieu, C. Samuelis, H. Knöckel, F. Masnou-Seeuws, and E. Tiemann, Observation of the long-range potential well of the (6)¹Σ_g⁺(3s + 5s) state of Na₂, *Eur. Phys. J. D* **26**, 173 (2003).
- [6] R. Kosloff and C. Cerjan, Dynamical atom/surface effects: Quantum mechanical scattering and desorption, *J. Chem. Phys.* **81**, 3722 (1984).
- [7] G. Jolicard and E. J. Austin, Optical potential stabilisation method for predicting resonance levels, *Chem. Phys. Lett.* **121**, 106 (1985).
- [8] R. Kosloff and D. Kosloff, Absorbing boundaries for wave propagation problems, *J. Comput. Phys.* **63**, 363 (1986).
- [9] D. Neuhauser and M. Baer, The time-dependent Schrödinger equation: Application of absorbing boundary conditions, *J. Chem. Phys.* **90**, 4351 (1989).
- [10] C. Leforestier and R. E. Wyatt, Optical potential for laser induced dissociation, *J. Chem. Phys.* **78**, 2334 (1983).
- [11] C. Leforestier and R. E. Wyatt, Role of Feshbach resonances in the infrared multiphoton dissociation of small molecules, *J. Chem. Phys.* **82**, 752 (1985).
- [12] R. D. Woods and D. S. Saxon, Diffuse surface optical model for nucleon-nuclei scattering, *Phys. Rev.* **95**, 577 (1954).
- [13] M. S. Child, Analysis of a complex absorbing barrier, *Mol. Phys.* **72**, 89 (1991).
- [14] J.-Y. Ge and J. Z. H. Zhang, Use of negative complex potential as absorbing potential, *J. Chem. Phys.* **108**, 1429 (1998).
- [15] A. N. Hussain and G. Roberts, Procedure for absorbing time-dependent wave functions at low kinetic energies and large bandwidths, *Phys. Rev. A* **63**, 012703 (2000).
- [16] N. Moiseyev, Derivations of universal exact complex absorption potentials by the generalized complex coordinate method, *J. Phys. B: At. Mol. Opt. Phys.* **31**, 1431 (1998).
- [17] R. Zavin, I. Vorobeichik, and N. Moiseyev, Motion of wavepackets using the smooth-exterior-scaling complex potential, *Chem. Phys. Lett.* **288**, 413 (1998).
- [18] B. Poirier and T. Carrington, Jr., Semiclassically optimized complex absorbing potentials of polynomial form. II. Complex case, *J. Chem. Phys.* **119**, 77 (2003).
- [19] O. Shemer, D. Brisker, and N. Moiseyev, Optimal reflection-free complex absorbing potentials for quantum propagation of wave packets, *Phys. Rev. A* **71**, 032716 (2005).
- [20] J.-Y. Ge and J. Z. H. Zhang, Channel-dependent complex absorbing potential for multi-channel scattering, *Chem. Phys. Lett.* **292**, 51 (1998).
- [21] Y. Yu and B. D. Esry, An optimized absorbing potential for ultrafast, strong-field problems, *J. Phys. B: At. Mol. Opt. Phys.* **51**, 095601 (2018).
- [22] Á. Vibók and G. G. Balint-Kurti, Parametrization of complex absorbing potentials for time-dependent quantum dynamics, *J. Phys. Chem.* **96**, 8712 (1992).
- [23] I. Schaefer and R. Kosloff, Optimization of high-order harmonic generation by optimal control theory: Ascending a functional landscape in extreme conditions, *Phys. Rev. A* **101**, 023407 (2020).
- [24] B. Poirier and T. Carrington, Semiclassically optimized complex absorbing potentials of polynomial form. I. Pure imaginary case, *J. Chem. Phys.* **118**, 17 (2003).
- [25] A. A. Silaev, A. A. Romanov, and N. V. Vvedenskii, Multi-hump potentials for efficient wave absorption in the numerical solution of the time-dependent Schrödinger equation, *J. Phys. B: At. Mol. Opt. Phys.* **51**, 065005 (2018).
- [26] S. Brouard, D. Macías, and J. G. Muga, Perfect absorbers for stationary and wavepacket scattering, *J. Phys. A: Math. Gen.* **27**, L439 (1994).
- [27] D. Macías, S. Brouard, and J. G. Muga, Optimization of absorbing potentials, *Chem. Phys. Lett.* **228**, 672 (1994).
- [28] D. E. Manolopoulos, Derivation and reflection properties of a transmission-free absorbing potential, *J. Chem. Phys.* **117**, 9552 (2002).
- [29] P. S. Julienne and F. H. Mies, Collisions of ultracold trapped atoms, *J. Opt. Soc. Am. B* **6**, 2257 (1989).
- [30] A. Mody, M. Haggerty, J. M. Doyle, and E. J. Heller, No-sticking effect and quantum reflection in ultracold collisions, *Phys. Rev. B* **64**, 085418 (2001).
- [31] C. Carraro and M. W. Cole, Quantum reflection, *Z. Phys. B* **98**, 319 (1995).
- [32] R. Côté, E. J. Heller, and A. Dalgarno, Quantum suppression of cold atom collisions, *Phys. Rev. A* **53**, 234 (1996).
- [33] M. B. Soley and E. J. Heller, Classical approach to collision complexes in ultracold chemical reactions, *Phys. Rev. A* **98**, 052702 (2018).
- [34] J. Petersen, E. Pollak, and S. Miret-Artes, Quantum threshold reflection is not a consequence of a region of the long-range attractive potential with rapidly varying de Broglie wavelength, *Phys. Rev. A* **97**, 042102 (2018).
- [35] J. M. Rost and E. J. Heller, Semiclassical scattering of charged particles, *J. Phys. B: At. Mol. Opt. Phys.* **27**, 1387 (1994).
- [36] P. Kustaanheimo and E. Stiefel, Perturbation theory of Kepler motion based on spinor regularization, *J. Reine Angew. Math.* **1965**, 204 (1965).
- [37] M. B. Soley, Escaping from an ultracold inferno: Classical and semiclassical mechanics near threshold, Ph.D. dissertation, Harvard University, Cambridge, MA, 2019.
- [38] M. B. Soley and E. J. Heller (unpublished).
- [39] N. T. Maitra and E. J. Heller, Semiclassical perturbation approach to quantum reflection, *Phys. Rev. A* **54**, 4763 (1996).
- [40] G. Wentzel, Eine Verallgemeinerung der Quantenbedingung für eine Zwecke der Wellenmechanik, *Z. Phys.* **38**, 518 (1926).
- [41] H. A. Kramers, Wellenmechanik und halbzahlige Quantisierung, *Z. Phys.* **39**, 828 (1926).
- [42] L. Brillouin, La mécanique ondulatoire de Schrödinger une method générale de resolution par approximations successives, *C. R. Hebd. Séances Acad. Sci.* **183**, 24 (1926).
- [43] L. Brillouin, Remarques sur la mécanique ondulatoire, *J. Phys. Radium* **7**, 353 (1926).

- [44] D. P. Clougherty and W. Kohn, Quantum theory of sticking, *Phys. Rev. B* **46**, 4921 (1992).
- [45] U. V. Riss and H.-D. Meyer, Calculation of resonance energies and widths using the complex absorbing potential method, *J. Phys. B: At. Mol. Opt. Phys.* **26**, 4503 (1993).
- [46] U. V. Riss and H. D. Meyer, Reflection-free complex absorbing potentials, *J. Phys. B: At. Mol. Opt. Phys.* **28**, 1475 (1995).
- [47] U. V. Riss and H.-D. Meyer, The transformative complex absorbing potential method: A bridge between complex absorbing potentials and smooth exterior scaling, *J. Phys. B: At. Mol. Opt. Phys.* **31**, 2279 (1998).
- [48] S. Falke, I. Sherstov, E. Tiemann, and C. Lisdat, The $A^1\Sigma_u^+$ state of K_2 up to the dissociation limit, *J. Chem. Phys.* **125**, 224303 (2006).
- [49] S. Ospelkaus, K.-K. Ni, D. Wang, M. H. G. de Miranda, B. Neyenhuis, G. Quéméner, P. S. Julienne, J. L. Bohn, D. S. Jin, and J. Ye, Quantum-state controlled chemical reactions of ultracold potassium-rubidium molecules, *Science* **327**, 853 (2010).
- [50] J. N. Byrd, J. A. Montgomery, Jr., and R. Côté, Structure and thermochemistry of K_2Rb , KRb_2 , and K_2Rb_2 , *Phys. Rev. A* **82**, 010502 (2010).
- [51] M. Born, Quantenmechanik der Stoßvorgänge, *Z. Phys.* **38**, 803 (1926).
- [52] L. D. Landau and E. M. Lifshitz, *Quantum Mechanics: Non-relativistic Theory*, 2nd ed. (Pergamon, New York, 1965), Vol. 3.
- [53] G. R. Satchler, The distorted-waves theory of direct nuclear reactions with spin-orbit effects, *Nucl. Phys.* **55**, 1 (1964).
- Correction:* The article title appearing in Ref. [34] was incorrect and has been fixed.